Journal of Hydrology: Regional Studies 8 (2016) 274–286

Contents lists available at ScienceDirect

Journal of Hydrology: Regional Studies

journal homepage: www.elsevier.com/locate/ejrh

Climate variability and irrigation impacts on streamflows in a Karst watershed—A systematic evaluation

Sarmistha Singh[a,*], Puneet Srivastava[a], Subhasis Mitra[a], Ash Abebe[b]

[a] Biosystems Engineering, Auburn University, Tom E. Corley Building, Auburn, AL 36849, USA
[b] Department of Mathematics & Statistics, Auburn University, 221 Parker Hall, Auburn, AL 36849, USA

ARTICLE INFO

Article history:
Received 12 April 2016
Received in revised form 15 June 2016
Accepted 1 July 2016

Keywords:
Streamflow
Baseflow
Irrigation
Climate variability
ENSO
JRFit

ABSTRACT

The study area is the Lower Flint River Basin which is at the center of water conflicts in the southeastern USA.

This study focuses on a systematic evaluation and separation of El Niño Southern Oscillation (ENSO) induced droughts and irrigation water withdrawal impacts on flow levels using a novel and powerful statistical technique, called JRFit. JRFit procedure was applied to quantify significant differences in streamflows, baseflows, and low flow statistics during non-irrigation (NI) and irrigation (IR) periods associated with ENSO phases.

The results indicate that overall streamflow levels have decreased by approximately 20% after the introduction of irrigation in the study area. Lowering of flow levels mainly occur during La Niña phases which gets exacerbated (decreased by 50%) during growing season of IR compared to NI periods. Flow duration curve analysis showed that the frequency of low flows has increased during IR period impairing aquatic ecosystem. This is the first time an elimination approach is used to separate and quantify the impacts of anthropogenic and climate signals on water resources. This approach avoids the need of using complex and data intensive groundwater/surface water models in studying climate-stream-aquifer interactions which can be replicated easily in other data scarce watersheds. This study provides useful information to policymakers to devise irrigation water withdrawal policies during La Niña growing seasons for maintaining flow levels in the study area.

1. Introduction

Natural ocean-atmospheric climate variability phenomena affect temperature and precipitation around the world and are also responsible for extreme events such as hurricanes, floods, droughts, and cold waves (IPCC, 2001; Seneviratne et al., 2012). Studies have found strong influence of climate variability phenomena on components of hydrologic cycle in many parts of the world. Therefore, it is important to understand and quantify the effects of climate variability phenomena on water resources to help mitigate their adverse effects on water resources. In addition to natural, short-term climate variability induced stresses on water resources, an ever growing global population with increasing need for irrigated agriculture is putting stress on freshwater bodies such as lakes, streams, and aquifers. In the past 50 years, the demand for water consumption for human use has increased by almost three-folds, and it is projected that by 2025 five out of eight people will be living under water scarce conditions across the world including the USA (Postel et al., 1996). Around the world, water

* Corresponding author.
E-mail address: szs0082@auburn.edu (S. Singh).

http://dx.doi.org/10.1016/j.ejrh.2016.07.001
2214-5818/

managers are facing challenges to meet the increasing water demands due to population growth, irrigated agriculture, and urban usage which gets exacerbated due to interannual climate variability. To be able to cope and better manage future water shortages resulting from climate variability-induced droughts and human-induced water scarcity, it is important to study the combined impact of anthropogenic factors and climatic oscillation on hydrology and their effects on water resources.

El Niño Southern Oscillation (ENSO), with a periodicity of 2–7 years, is the fluctuation in sea-surface temperature (SST) caused by the interaction between large-scale ocean and atmospheric circulations in the equatorial Pacific Ocean. ENSO has three phases such as El Niño, La Niña and Neutral. The terms "El Niño" and "La Niña" refer to the warming and cooling of SST off the shores of the West Coast of South America that leads to changes in climatic conditions around the world (Quinn, 1994; Aceituno, 1992). ENSO is one of the major modes of climate variability affecting temperature and precipitation around the world (Diaz and Markgraf, 1992; Chiew et al., 1998; Keener et al., 2007; Roy, 2006). Several studies have found that ENSO has a strong influence on droughts, streamflow, groundwater, flood frequency, monsoon, water quality, and crop yield in different parts of the world (Kahya and Dracup, 1993; Chiew et al., 1998; Rajagopalan and Lall, 1998; McCabe and Dettinger 1999; Piechota and Dracup, 1999; Kulkarni, 2000; Hansen et al., 2001; Tootle et al., 2005; Roy, 2006; Keener et al., 2007; Gurdak et al., 2007; Singh et al., 2015).

Moreover, other studies have shown that ENSO exhibits strong teleconnections with precipitation, streamflow, baseflow and groundwater in the southeastern USA (Singh et al., 2015; Mitra et al., 2014; Piechota and Dracup, 1996; Tootle et al., 2005; Mearns et al., 2003; Kiladis and Diaz, 1989; Hansen et al., 2001; Enfield et al., 2001; Johnson et al., 2013; Schmidt and Luther, 2002). This region often suffers from low surface water availability due to frequent occurrences of La Niña, which brings warm and dry conditions between the months of October and April (Kiladis and Diaz, 1989; Hansen and Maul, 1991; Schmidt and Luther, 2002; Mearns et al., 2003), making the region vulnerable to ENSO-induced droughts. Furthermore, water shortages in this region get exacerbated due to high evaporation rates during summer months and increased demand for water due to growth in population, urbanization and irrigated agriculture, especially in the past few decades. The Southeast has experienced recurring droughts that have caused losses in agricultural productivity, prompted water use restrictions on municipal and irrigated waters uses, and induced interstate water conflicts. This combined stress of climate variability-induced droughts, population growth, and irrigation withdrawal on water resources has led to the so-called "Tri-State Water Conflict" among the neighboring states of Georgia, Alabama and Florida (Jordan and Wolf, 2006). This conflict has been marked by costly, time consuming and ongoing litigations where the sparring parties have failed to reach a common ground on the allocation of water resources of the Apalachicola-Chattahoochee-Flint (ACF) River Basin (Fig. 1), thereby making the ACF one of the most contentious river basins in the United States. The freshwater resources of the ACF provide support to rapidly growing population; urban sprawl; industrial, municipal and rural water supplies; power generation; irrigated agriculture; shellfish industry; and estuarine ecosystem. One of the major issues related to the ongoing conflict is the irrigation-induced lowering of flow levels in the Flint River.

Agriculture in the Lower Flint River (LFR) Basin (in southwest Georgia) is heavily dependent on irrigation water withdrawals from surface and groundwater sources. Since the mid 1970's, groundwater withdrawals for irrigation has increased dramatically in the LFR Basin (Fig. 2) due to extensive installation of center pivot irrigation systems (Hicks et al., 1987; Pierce et al., 1984) where the ratio of groundwater sites to surface water sites is 5:1. During a drought year (typically caused by La Niña), groundwater withdrawal from the Upper Floridan Aquifer (UFA), which is the major groundwater bearing unit in the area, can run into hundreds of millions of gallons per day. The flow in the LFR is hydro-geologically connected with UFA through direct connections with many sinkhole ponds, karst sinks, conduits and trough incised streambeds, and indirect connections through vertical leakage from overburden (Mosner, 2002; Opsahl et al., 2007).

The hydrologic connectivity/interaction of groundwater with surface water has become a topic of interest among researchers worldwide since it supports baseflow and serves as a major water resource unit (Shah et al., 2000; Woessner, 2000; Stanford and Ward, 1993; Winter et al., 1998; Boulton and Hancock, 2006). Intensive groundwater withdrawal near stream channels have been linked to alterations in the quantity and quality of surface waters, which leads to changes in channel morphology, altered stream temperature, lower assimilative capacity, reduced nutrient loading to downstream communities (Pringle and Triska, 2000; Bunn and Arthington, 2002), and threats to aquatic biota including federally-protected mussel species (Golladay et al., 2004). Therefore, this study aims to understand the relationships between droughts, irrigation water withdrawals, and streamflow levels in the study area. To achieve the goal of this study, streamflows and baseflows for the non-irrigation and irrigation periods were compared with the ENSO phases. The comprehensive outcomes of this study can be used to help the state of Georgia better manage drought and irrigation induced streamflow reductions in the LFR.

2. Methodology

To attain the research goal, the nonparametric Joint Rank Fit (JRFit) procedure (Kloke et al., 2009) was used to test and estimate the ENSO-induced drought and irrigation impacts on streamflow, baseflow, one-day, and seven-day low flows levels. Additionally, flow duration curves for the lower Flint River were created and compared for non-irrigation (NI) and irrigation (IR) periods.

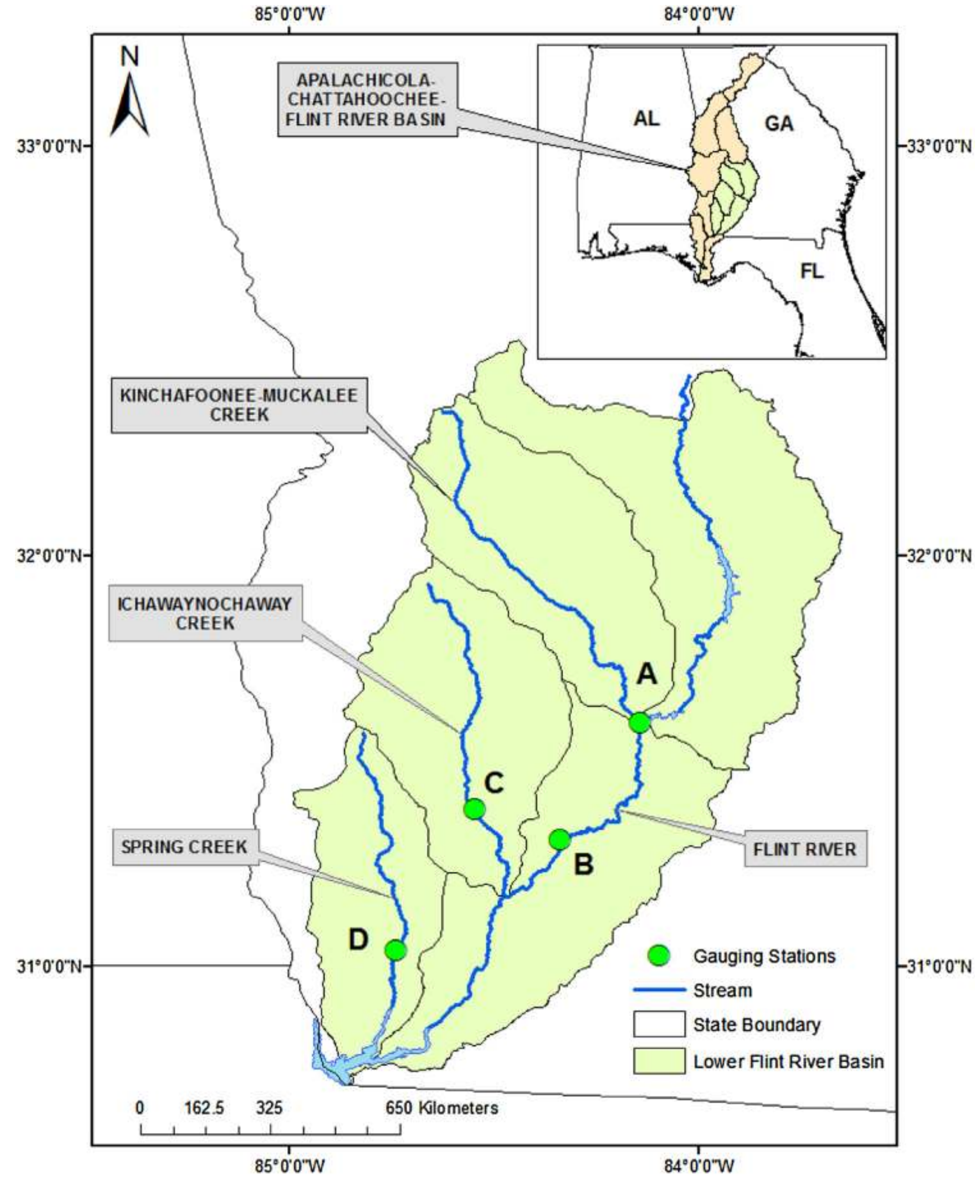

Fig. 1. The Lower Flint River (LFR) Basin showing the critical sub-watersheds. The stream flow gaging stations selected for this study are shown as green circles.

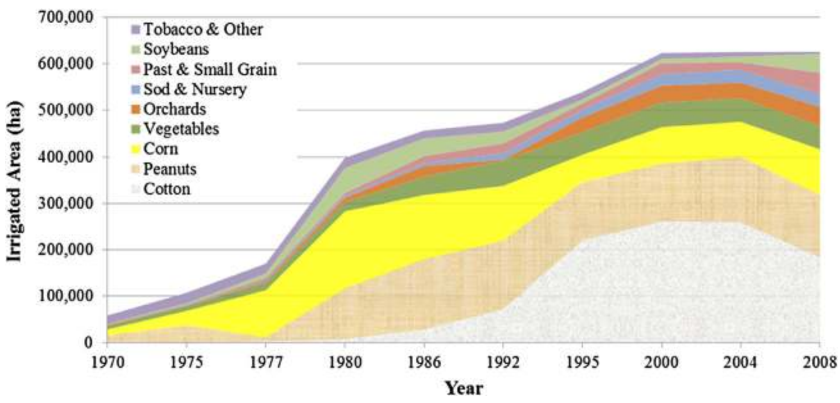

Fig. 2. Increase in irrigated acreage in the Lower Flint River Basin (Harrison, 2009).

Table 1
Selected streamflow gaging stations used in this study showing the USGS station ID, location, their assigned names used in the manuscript and their respective data date ranges.

Station ID	Location	Latitude	Longitude	Assigned Name	Data date Range (Year)
02352500	Flint River, Albany, GA	31.594	−84.144	A	1930–2014
02353000	Flint River, Newton, GA	31.307	−84.339	B	1957–2014
02353500	Ichawaynochaway Creek, Milford, GA	31.383	−84.546	C	1940–2014
02357000	Spring Creek, Iron City, GA	31.040	−84.740	D	1938–1970 and 1983–2014

2.1. Study area

The study area is the LFR Basin located in southwest Georgia (Fig. 1). The climate in the LFR is hot and humid with long summers (temperature ranges from 18 to 35 °C) and mild winters (temperature ranges from 2 to 13 °C) (Jones and Torak, 2006). The average annual precipitation is 1200 mm, which varies spatially across the region (Jones and Torak, 2006; Rugel et al., 2011).

The ACF river basin contains karstic and fluvial plains, and predominantly contains karst limestone which contributes to the exchange of groundwater and surface water in this stream-lake-aquifer flow system. The tributaries and principal rivers of the lower Flint are hydraulically connected to UFA, which is the principal water bearing hydrologic unit in the study area. The land use of the LFR is largely in agriculture (50%) with row crop farming of cotton, corn, wheat, soybeans, and peanuts. The farming systems in the LFR are primarily supported by center pivot irrigation which withdraws water from surface and groundwater (i.e., UFA) resources.

2.2. Data

To understand the impact of irrigation and drought on the Flint River flow levels, streamflow data from four United States Geological Survey (USGS) gaging stations, and climate variability (ENSO) data from the National Oceanic and Atmospheric Administration (NOAA), were used. Historic rainfall data were also collected from NOAA for the cities of Albany and Tifton to analyze changes in rainfall amounts between NI to IR periods.

2.2.1. Climate variability (ENSO) data

There are several indices that are universally accepted for the identification of ENSO cycles (Tootle et al., 2005). In general, ENSO indices (Beebee and Manga, 2004; Tootle et al., 2005) are calculated based on atmospheric observations such as the Southern Oscillation Index (SOI) (Troup, 1965; Chen, 1982; Ropelewski and Jones, 1987), based on sea surface temperatures (SST) (e.g., the Niño 3.4 index) (Trenberth, 1997; Trenberth and Stepaniak, 2001), and combination of both ocean and atmospheric parameters such as the Multivariate ENSO Index (MEI) (Wolter and Timlin, 1993). In this study, the Niño 3.4 SST index (ERSST.v3b), obtained from the NOAA Climate Prediction Center (CPC), was used to define ENSO phases and durations. The Niño 3.4 index is based on the SST anomalies in the Niño 3.4 region (5°N–5°S, 120°–170°W). The Niño 3.4 index value of above +0.5 °C corresponds to the occurrence of an El Niño event and a value below −0.5 °C represents a La Niña event. When Niño 3.4 index value is between −0.5 °C and +0.5 °C, ENSO is considered to be in Neutral phase.

2.2.2. Streamflow data

Four USGS stations (Fig. 1) were selected based on the length of data availability. Two stations, namely A and B, are on the Flint River and the other two are on the tributaries Ichawaynochaway Creek (C) and Spring Creek (D) (Table 1 and Fig. 1).

Ichawaynochaway Creek, a fifth-order tributary, flows to the Flint River, while Spring Creek, a third-order tributary of the Flint River, flows directly to Lake Seminole. At Lake Seminole, the Flint and Chattahoochee Rivers join to form the Apalachicola River. Daily streamflow data in cubic feet per second were obtained from these USGS gaging stations with historical data of approximately 75 years, except for station D (Table 1). The daily values were changed into monthly cubic meters per second (m^3/s) and were sorted according to ENSO phases and growing seasons.

2.2.3. Baseflow data

Baseflow was separated from daily streamflow data using Web-based Hydrograph Analysis Tool (WHAT). This tool uses two digital filter methods, BFLOW and Eckhardt (Lim et al., 2005), for baseflow separation. In this study, Eckhardt filter method with baseflow index 0.9 (Eckhardt, 2005) was used for baseflow separation since it is used for perennial rivers (Lim et al., 2005). The equation used for the Eckhardt filter method is shown below:

$$b_t = \frac{(1 - BFI_{max})\alpha b_{t-1} + (1 - \alpha) BFI_{max} Q_t}{1 - \alpha BFI_{max}} \quad (1)$$

where, BFI_{max} is the maximum value of long term ratio of base flow to total streamflow; b_{t-1} is the filtered base flow at the time step t-1; α is the filter parameter; b_t is the filtered base flow at the time step t and Q_t is the total streamflow at the time step t.

2.3. Statistical method

Streamflow/baseflow data exhibit more or less similar patterns each month of every year; that is, they are clustered by month. Therefore, the nonparametric JRFit (Kloke et al., 2009) procedure, an extension of the Wilcoxon rank-sum procedure for the analysis of clustered correlated data, was used in this study. Since flow data are likely to contain outliers and/or skewness, the Wilcoxon rank-sum method has been commonly applied in the literature for the comparison of median flows under different conditions (Tootle et al., 2005; Johnson et al., 2013). The Wilcoxon rank-sum, or its extension the Wilcoxon rank-regression, are not appropriate for cluster-correlated responses since cluster correlation in the responses inflates their estimation standard errors. On the other hand, JRFit, uses joint ranking to obtain unbiased estimates of the effect sizes and standard errors for the cluster-correlated data, hence is a powerful nonparametric alternative to linear mixed effect models for data with cluster-correlated responses. Accounting for within month clustering also accounts for seasonality, a phenomenon that occurs on a coarser scale. Kloke et al. (2009) show that the JRFit procedure minimizes the metric given in Jaeckel (1972). While this metric is pseudo-norm instead of a norm, it generates estimation geometry similar to least squares minimization (McKean and Schrader, 1980) but is less sensitive to unusual perturbations in the data than the least squares or maximum likelihood methods. Kloke et al. (2009) also established that the JRFit procedure results in an unbiased and efficient estimator of the slope parameter with an asymptotic Gaussian distribution. With the exception of a condition on cluster structure, the assumptions needed for their results are the standard regularity conditions for the asymptotic normality of maximum likelihood estimators (Lehmann and Casella, 1998) as well as the conditions needed for asymptotic normality of the Wilcoxon rank-sum procedure (Hettmansperger and McKean, 2011). The assumption on the clusters is that distinct clusters are independent and that the within-cluster correlation is exchangeable. In this study, this means that observations from different months are independent however, observations from the same month of different years are equally correlated. The asymptotic Gaussian distribution may be used to construct efficient Wald-type significance tests of the model parameters without segregating the data resulting in powerful tests (Kloke et al., 2009; Hettmansperger and McKean, 2011). The tests are performed by creating a ratio of the estimated slope to the estimated standard error (formed using a consistent plug-in estimate of the asymptotic variance) which are compared to standard Gaussian distribution tails to obtain *p*-values for assessing statistical significance. The following general linear regression model was used to estimate the effect of climate variability phenomenon (ENSO) or irrigation (X) on streamflow/baseflow (Y)

$$Y = \beta_0 + \beta_1 X + \varepsilon, \tag{2}$$

where, $X = 0$ and $X = 1$ represent non-irrigation (NI) and irrigation (IR) periods, and ε represents random errors. The condition on the cluster correlation given by Kloke et al. (2009) implies that the error correlation matrix is block-diagonal with blocks representing months and each block is a compound-symmetric (exchangeable) matrix. The value of β_1 represents the change in flow levels due to change of phase from NI to IR. The model implies that responses in the same month have the same underlying year-to-year correlation; however, two responses from the same month from an NI year and an IR year, respectively, differ by β_1. We use the same model (2) for comparing NI and IR within ENSO phases or growing/non-growing seasons.

2.3.1. Non-irrigation and irrigation flow comparison

In this study, streamflow/baseflow data sets were divided into two time periods non-irrigation (NI; ≤year 1975) and irrigation (IR; >year 1975) periods. The NI period for the Spring Creek gaging station was defined from 1940 to 1969 and IR period from 1983 to 2014 due to unavailability of data during the missing period (from 1971 to 1982) (Table 1). The significant difference in median streamflows/baseflows for each gaging station was tested and estimated using the JRFit procedure. The percentage changes in estimated medians of streamflows/baseflows were calculated between the NI and IR periods. The significant difference of median streamflows/baseflows between the NI and IR periods during El Niño and La Niña phases were also estimated to understand the individual impact of climate variability, and the combined impact of irrigation and climate variability cycles on the LFR flows. To verify the effect of irrigation on streamflow/baseflow levels, growing and non-growing season analysis were conducted for the overall and the ENSO phases associated with the NI and IR periods. Growing season was defined as the months from April to October and the remaining months were considered as the non-growing season. The overall median streamflow/baseflow levels of growing and non-growing seasons were compared for NI and IR periods using the JRFit procedure.

2.3.2. One-day and seven-day low flows

In this study, 1- and 7-day low flows were analyzed for the NI and IR periods. One-day low flow is defined as the lowest streamflow in a given month and 7-day low flow is the lowest seven-day running average streamflow for that month. The significant differences in median low flows for NI and IR periods were tested and quantified using the JRFit procedure. The significant differences in median low flows between NI and IR periods during El Niño and La Niña phases were also estimated to understand individual impacts ENSO phases, and the combined impacts of irrigation and climate variability cycles on low flows.

Table 2
JRFit estimated median monthly streamflows (m^3/s), *p*-values and percentage differences in streamflows during the non-irrigation (NI) and irrigation (IR) periods.

Station ID	NI	IR	N_{NI}/N_{IR}^*	% difference NI to IR	p- value
A	124.48	103.89	540/480	−17	0.000
B	150.48	120.59	216/480	−20	0.000
C	17.23	13.87	432/468	−19	0.000
D	7.50	6.58	396/384	−12	0.036

N_{NI}/N_{IR}^* = number of observations during NI/number of observations during IR.

Table 3
JRFit estimated median monthly precipitation (mm) and *p*-values for during NI and IR periods.

Precipitation Gaging Stations (Years)	Albany (1950–2014)			Tifton (1930–2014)		
	NI	IR	p- value	NI	IR	p- value
Overall	93.9	95.8	0.704	86.2	87.3	0.836
El Niño	102.8	106.7	0.630	96.4	103.2	0.441
La Niña	83.4	78.2	0.533	73.2	72.9	0.972

2.3.3. Flow duration curve analysis

Flow duration curve (FDC) is a cumulative frequency curve that shows the percent of time a flow was equaled or exceeded without regard to the sequence of occurrence during a given period. FDC has different intervals that can be used as a general indicator of the probability of hydrologic conditions such as dry or wet. The intervals are categorized into different zones such as the moist, mid-range, and dry zones at the quartiles (25th, 50th, and 75th percentiles, respectively). In this study, FDCs were constructed for the NI and IR daily flows and analyzed graphically for each station.

3. Results and discussion

3.1. Streamflow analysis

A comparison of NI and IR periods was performed on monthly median streamflows using the JRFit procedure to determine if there were significant streamflow depletions during the IR period as compared to the NI period. The results of the JRFit analysis for the NI and IR periods are presented in Table 2. It was found that the differences in median streamflows between the NI and IR periods were highly significant ($p < 0.01$) for all the stations except for station D, which was not highly significant but significant ($p < 0.05$) nonetheless.

Overall, median streamflows decreased by approximately 20% during the IR period (Table 2). This might be due to the combined effect of water withdrawal from UFA and climatic influences such as decrease in rainfall amounts and occurrence of severe droughts during the IR period. To examine if the changes in median streamflows were caused by shifts in precipitation patterns, precipitation data for the IR and NI periods were also analyzed. Comparison of precipitation data for the NI and IR periods suggested that precipitation did not exhibit a significant change during the respective periods and the changes in the streamflow levels are due to human interactions only. Also, the JRFit analysis of precipitation data for the El Niño and La Niña phases suggested no significant difference ($p > 0.05$) between NI and IR period median rainfall patterns for the phases of ENSO (Table 3).

Similar results have also been reported by several researchers showing that no significant differences in rainfall amounts were found from 1938 to 2005 in the southeastern USA (Rose, 2009; Seager et al., 2009) and the recent droughts are similar to historic droughts, thus suggesting that the current water shortages are mainly due to increased water demand in this region (Seager et al., 2009; Rugel et al., 2011). Although repeated droughts have occurred in the last decade, the study done by Rugel et al. (2011) on Palmer Drought Severity Index (PDSI) and precipitation showed that there has been no reduction in average precipitation or any increase in the severity of drought during irrigation years.

Since the La Niña and El Niño phase precipitation pattern and amount have not changed during the NI and IR periods, the median streamflow levels associated with El Niño and La Niña periods were analyzed to quantify the effect of irrigation during the respective ENSO phases. The results pertaining to the comparison of median streamflows during the NI and IR periods for the El Niño and La Niña phases are presented in Table 4. The results showed no significant differences between the median streamflows in NI and IR periods associated with El Niño due to small irrigation withdrawal during the El Niño phases (Table 4). However, except for station D ($p > 0.05$), significant differences ($p \leq 0.01$) in median streamflows during the NI and IR periods were found when they were associated with La Niña events (Table 4). The median streamflow levels have reduced by as much as 34% (station B) during the IR period as compared to the NI period (Table 4) during La Niña phases (droughts). This indicates that perhaps irrigation water withdrawal from the Flint River during droughts are responsible for lowering of flow levels.

Table 4
JRFit estimated median monthly streamflows (m^3/s), *p*-values, and percentage differences in streamflows from NI to IR periods associated with phases of ENSO.

Station ID	El Niño					La Niña				
	NI	IR	N_{NI}/N_{IR}	% change NI to IR	p-value	NI	IR	N_{NI}/N_{IR}	% change NI to IR	p-value
A	135.81	135.00	139/115	−1	0.901	104.96	92.06	140/128	−12	0.01
B	144.03	148.43	74/115	3	0.479	162.32	106.56	46/128	−34	0.00
C	17.27	17.77	123/115	3	0.543	15.63	11.68	129/116	−25	0.00
D	8.25	10.28	113/95	25	0.126	4.20	3.56	97/112	−15	0.30

Table 5
JRFit estimated median monthly baseflow (m^3/s), *p*-values and percentage differences in baseflows from NI to IR periods.

Station ID	NI	IR	% difference NI to IR	p- value
A	84.96	71.94	−15	0.000
B	110.31	89.21	−19	0.000
C	12.90	10.16	−21	0.000
D	5.60	4.77	−15	0.007

Table 6
JRFit estimated median monthly baseflows (m^3/s), *p*-values and percentage differences in median baseflows associated with phases of ENSO for the NI and IR periods.

Station ID	El Niño				La Niña			
	NI	IR	% change NI to IR	p-value	NI	IR	% change NI to IR	p-value
A	87.48	87.72	0	0.953	71.60	62.70	−12	0.006
B	99.87	103.52	4	0.353	118.59	78.73	−34	0.000
C	12.39	12.19	−2	0.740	12.14	9.09	−25	0.001
D	5.59	6.84	22	0.169	3.08	2.51	−18	0.182

Table 7
JRFit estimated median monthly 1-day low flows (m^3/s), *p*-values and percentage differences in 1-day low flows from NI to IR periods.

Station ID	NI	IR	% difference NI to IR	p- value
A	58.16	51.14	−12	0.003
B	84.51	69.52	−18	0.000
C	10.89	8.11	−25	0.000
D	3.89	2.94	−24	0.000

3.2. Baseflow analysis

Similarly, baseflow analyses were performed to account for the stream-aquifer interaction response to groundwater extractions (Table 5). Highly significant differences between NI and IR period median baseflows ($p < 0.01$) were found across all stations, and median baseflow levels were found to be reduced by approximately 18% during the IR period as compared to the NI period (Table 5). Rugel et al. (2011) also found similar patterns of decrease in baseflow in the LFR basin.

Similar to streamflow analysis, baseflow results also showed no significant differences between the median streamflows in NI and IR periods when associated with El Niño phase. However, except for station D ($p > 0.05$), which might be due to data availability for a shorter period, the differences between the median streamflows were found to be highly significant ($p \leq 0.01$) during La Niña phases (Table 6). Recent studies done by Jones and Torak (2006) have also suggested that groundwater withdrawals have lowered potentiometric surface of groundwater by decreasing potential recharge, which explains the results found in Tables 5 and 6.

3.3. 1-Day and 7-day low flow analysis

The results pertaining to the comparison of the NI and IR periods for 1-day and 7-day low flows are presented in Tables 7 and 8, respectively. Overall, 1-day and 7-day median low flows reduced significantly ($p < 0.01$) during the IR period for all the gauges by approximately 20% and 22%, respectively (Tables 7 and 8).

Except for station B (which was significant at a level of 5%), analysis of 1-day and 7-day low flows showed no significant difference between NI and IR period low flows during El Niño (Table 9 and 10). Similar to streamflow and baseflow results, except for station D (which is only marginally significant, likely because of the reason mentioned earlier), 1-day low flow values were substantially lower ($p < 0.05$) during the IR period when associated with La Niña phase (Table 9). One-day low flow values during La Niña phases were lower than the overall 1-day low flow values (Table 9). Overall, 1-day low flow value

Table 8
JRFit estimated median monthly 7-day low flows (m^3/s), *p*-values and percentage differences in seven-day low flows during NI and IR periods.

Station ID	NI	IR	% difference NI to IR	p- value
A	79.73	63.92	−20	0.000
B	103.66	81.37	−22	0.000
C	11.60	8.80	−24	0.000
D	4.13	3.19	−23	0.000

Table 9
JRFit estimated median monthly 1-day low flows (m^3/s), *p*-values and percentage differences in 1-day low flows associated with phases of ENSO for the NI and IR periods.

Station ID	El Niño				La Niña			
	NI	IR	% change NI to IR	p-value	NI	IR	% change NI to IR	p-value
A	57.30	58.33	2	0.712	49.57	45.29	−9	0.04
B	69.94	79.33	13	0.015	90.90	64.45	−29	0.00
C	10.39	9.81	−6	0.282	10.34	7.50	−27	0.00
D	3.92	4.42	13	0.456	2.49	1.88	−24	0.07

Table 10
JRFit estimated median monthly 7-day low flows (m^3/s), *p*-values and percentage differences in 7-day low flows associated with phases of ENSO for the NI and IR periods.

Station ID	El Niño				La Niña			
	NI	IR	% change NI to IR	p-value	NI	IR	% change NI to IR	p-value
A	80.71	77.55	−4	0.449	71.69	60.02	−16	0.00
B	95.87	96.26	0	0.934	115.77	76.90	−34	0.00
C	10.98	10.54	−4	0.524	11.15	8.26	−26	0.00
D	4.23	4.88	15	0.394	2.62	2.03	−22	0.12

Table 11
JRFit estimated median monthly streamflows (m^3/s), *p*-values and percentage differences in streamflows from NI to IR periods associated with non-growing and growing seasons.

Station ID	Non-Growing					Growing				
	NI	IR	N_{NI}/N_{IR}	% change NI to IR	p-value	NI	IR	N_{NI}/N_{IR}	% change NI to IR	p-value
A	180.58	169.77	230/195	−5.99	0.093	105.83	79.66	322/273	−24.74	0.000
B	208.86	182.46	90/200	−12.64	0.073	130.12	96.82	126/280	−25.59	0.000
C	23.81	22.06	180/195	−7.36	0.013	14.97	10.86	252/273	−27.47	0.000
D	11.12	12.12	165/160	9.02	0.279	6.31	4.55	231/224	−27.86	0.001

for station B during IR period was 18% lower than the NI period (Table 7), which further reduced by 29% (approximately one-third of 1-day low flow) during La Niña phases in the IR period (Table 9).

Similar to 1 day low flows, the differences between the median 7-day low flows in NI and IR periods were not significant during El Niño phase. However, highly significant differences were found during La Niña ($p < 0.01$) for all stations except station D ($p > 0.05$) (Table 10). Moreover, overall 7-day low flow value for station B during the IR period was 22% lower than the NI period (Table 8), and low flow levels further reduced by 34% during La Niña phases associated with IR period as compared to the NI period (Table 10). The above results show that pumping during droughts can have significant impact on 1-day and 7-day low flows and have the potential to impact the integrity of streams in this region.

The JRFit estimated median monthly streamflows, baseflows, 1-day and 7-day low flows are presented in Fig. 3. It was found that overall and La Niña flows during irrigation period have reduced substantially for all the stations. However, flows have not changed during the El Niño phase (Fig. 3). Fig. 3 also shows that flows during La Niña have substantially reduced in the IR period, which suggests that drought and irrigation water withdrawal during droughts from the aquifer leads to decrease flow levels during IR periods.

3.4. Growing and non-growing season analysis

3.4.1. Streamflow analysis

The results of the JRFit estimation comparing the NI and IR periods during non-growing and growing seasons are presented in Table 11. Except for station C, during non-growing seasons, marginal or no significant differences were found between median NI and IR period streamflows (Table 11). However, across all stations, highly significant differences ($p < 0.01$) were found for growing season median streamflows for the NI and IR periods, with streamflow levels decreaseing by approximately 26% during IR periods (Table 11).

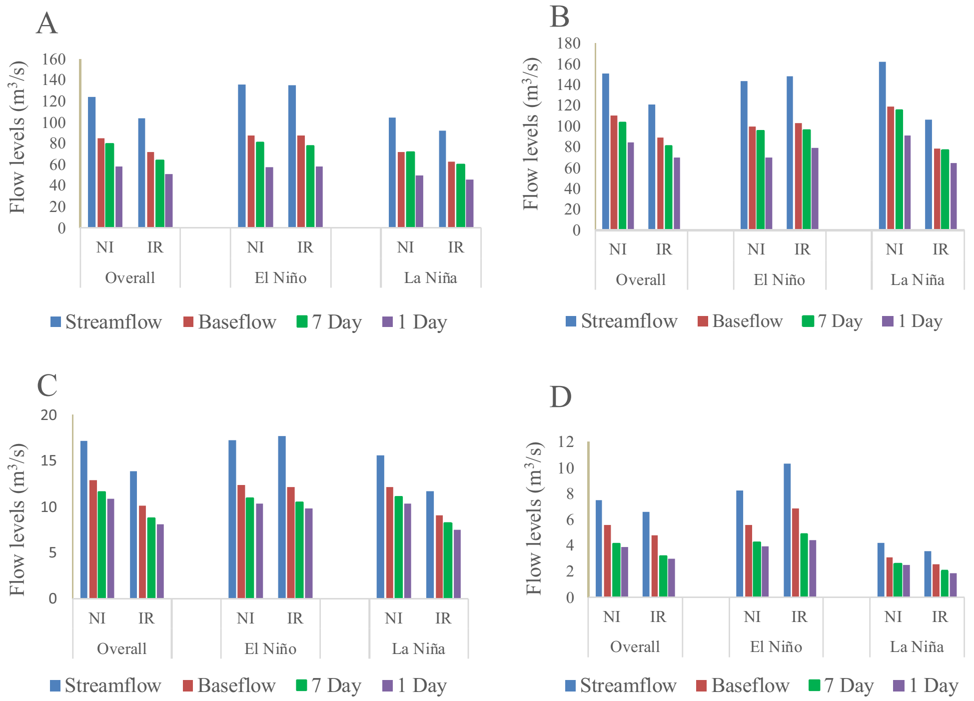

Fig. 3. JRFit estimated median monthly streamflows, baseflows, 1-day and 7-day low flows for stations A–D.

Table 12
JRFit estimated median monthly streamflows (m^3/s), *p*-values and percentage differences in streamflows from NI to IR periods associated with non-growing season for the phases of ENSO.

Station ID	El Niño					La Niña				
	NI	IR	N_{NI}/N_{IR}	% change NI to IR	p-value	NI	IR	N_{NI}/N_{IR}	% change NI to IR	p-value
A	195.04	216.79	63/54	11.15	0.055	123.71	125.87	66/64	1.75	0.823
B	192.09	217.12	32/54	13.03	0.215	205.81	151.98	18/69	−26.15	0.101
C	22.21	25.56	55/54	15.09	0.019	17.75	15.79	56/64	−11.08	0.086
D	12.54	21.23	51/44	69.28	0.006	3.95	5.33	43/61	34.96	0.173

Table 13
JRFit estimated median monthly streamflows (m^3/s), *p*-values and percentage differences in streamflows from NI to IR periods associated with growing season for the phases of ENSO.

Station ID	El Niño					La Niña				
	NI	IR	N_{NI}/N_{IR}	% change NI to IR	p-value	NI	IR	N_{NI}/N_{IR}	% change NI to IR	p-value
A	101.62	88.71	76/61	−12.71	0.026	93.69	63.34	86/52	−32.40	0.000
B	120.00	106.70	42/61	−11.08	0.067	155.01	75.36	28/59	−51.39	0.000
C	13.12	11.71	68/61	−10.76	0.127	14.65	8.07	73/52	−44.90	0.001
D	5.68	5.98	62/51	5.29	0.606	4.40	2.07	54/51	−52.97	0.001

The results of the JRFit estimation comparing the NI and IR periods during ENSO phases associated with non-growing seasons are presented in Table 12. No significant differences were observed during La Niña for all the stations. During El Niño, no significant difference were observed for the stations A and B (Table 12). This suggests that streamflow levels in non-growing seasons do not vary significantly between NI and IR periods even during La Niña phases.

However, interestingly, during the growing season when NI and IR periods were compared, except for station A significant ($p < 0.05$), no significant ($p > 0.05$) differences were observed between the median streamflows associated with El Niño phase (Table 13). However, the differences between the median streamflows of NI and IR periods were found to be highly significant ($p < 0.01$) when associated with La Niña phase (Table 13). During the La Niña cycle, except for station A (which were approximately 30% lower), streamflow levels were approximately 50% lower in the IR period. Comparison of the results in Tables 12 and 13 suggests that streamflow levels in the LFR and its tributaries are being impacted by irrigation water withdrawal, and streamflow levels in certain stream sections have reduced by as much as 50% since the introduction of irrigation in the mid 1970's.

Table 14
JRFit estimated median monthly baseflows (m^3/s), *p*-values and percentage differences in baseflows from NI to IR periods associated with non-growing and growing seasons.

Station ID	Non-Growing				Growing			
	NI	IR	% change NI to IR	p-value	NI	IR	% change NI to IR	p-value
A	121.73	113.64	−6.65	0.127	72.19	56.19	−22.16	0.000
B	147.87	130.63	−11.66	0.081	97.86	74.70	−23.66	0.000
C	16.87	15.43	−8.55	0.047	11.40	8.01	−29.72	0.000
D	7.24	7.64	5.61	0.449	5.07	3.61	−28.81	0.000

Table 15
JRFit estimated median monthly baseflows (m^3/s), *p*-values and percentage differences in baseflows from NI to IR periods associated with non-growing season for the phases of ENSO.

Station ID	El Niño				La Niña			
	NI	IR	% change NI to IR	p-value	NI	IR	% change NI to IR	p-value
A	133.29	146.64	10.02	0.093	85.39	86.24	0.99	0.893
B	139.13	151.02	8.54	0.199	127.19	103.12	−18.92	0.282
C	17.47	19.57	11.97	0.025	13.47	12.18	−9.57	0.283
D	9.25	13.59	46.90	0.077	2.93	3.82	30.36	0.087

Table 16
JRFit estimated median monthly baseflows (m^3/s), *p*-values and percentage differences in baseflows from NI to IR periods associated with growing season for the phases of ENSO.

Station ID	El Niño				La Niña			
	NI	IR	% change NI to IR	p-value	NI	IR	% change NI to IR	p-value
A	66.48	60.38	−9.18	0.059	63.31	43.87	−30.70	0.000
B	83.68	76.79	−8.23	0.067	112.47	55.50	−50.65	0.001
C	10.18	8.63	−15.22	0.011	11.20	6.16	−45.01	0.001
D	4.27	4.19	−1.89	0.807	3.66	1.78	−51.47	0.000

3.4.2. Baseflow analysis

Similar to streamflow analysis, baseflow levels also show significant differences between NI and IR periods during growing season and, except for the station C ($p < 0.05$), show no significant difference during non-growing season (Table 14). During non-growing seasons, no significant differences were observed between NI and IR periods associated with La Niña (across all the stations) and El Niño (except for station C) (Table 15). During growing seasons, except for station C, no significant differences were observed between NI and IR periods associated with El Niño.

However, highly significant differences in median baseflows were found between NI and IR periods associated with La Niña (Table 16). Moreover, overall baseflow levels during growing seasons have decreased substantially by approximately 26% (Table 14) in the IR period, which further lowered to approximately 50% during La Niña (Table 16). These results again suggest that stream-aquifer interaction gets affected by irrigation during droughts.

3.5. Flow duration analysis (FDC)

Flow duration curves were produced from the NI and IP period daily flows for all the gaging stations and are presented in Fig. 4. FDCs showed that 80% exceedance flows have dropped substantially for all the stations (Fig. 4). This suggests that low flows have been impacted and have reduced substantially during the IR period. However, high flows and above first quartile flows were identical during the NI and IR periods (Fig. 4).

The FDC suggests that, in the IR period, the occurrence of low flows have increased substantially as compared to the NI period. The gaging stations C and D suggests that tributary reaches are more severely affected by agricultural irrigation withdrawal since the FDC analysis shows that at times low flows have reduced to zero during the IR period, which was not the case during NI period (Fig. 4(C) and (D)). The results from the FDC analysis shows that irrigation water withdrawal affects the tributaries of the LFR more severely than the main Flint River since flow ranges in the tributaries are far less than the main Flint River. And, hence, any increase in irrigation can lead to certain portion of the streams becoming dry. Low flows are of utmost importance for the assimilation of waste and for the protection of river biota. Low flow levels leads to portions of a channel going dry. During such conditions, aquatic animals try to concentrate in pools where they are more vulnerable to aquatic and terrestrial predators (especially birds and raccoons). Aquatic animals that are unable to move to pool perish on dry stream beds (USFWS and EPA, 1999). Extremely low water levels during summer months are also associated with higher than normal water temperatures and low dissolved oxygen levels causing further stress to river flora and fauna.

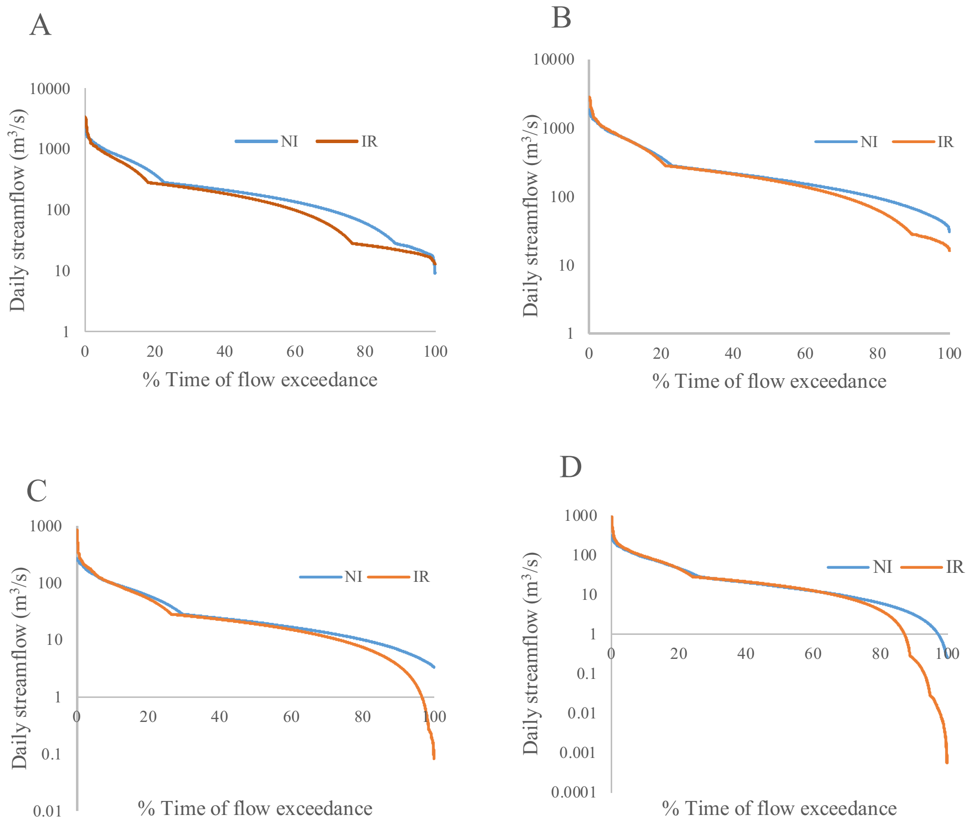

Fig. 4. Flow duration curves for the NI and IR periods for stations A–D.

4. Conclusions

This study quantified the impact of ENSO-induced droughts and irrigation water withdrawals on flow levels of the LFR using the non-parametric JRFit procedure. The results indicated that the groundwater withdrawals from the UFA in the LFR Basin has resulted in decreased streamflow/baseflow in the LFR and its tributaries. Especially during droughts (La Niña phases), when groundwater levels are already low (Mitra et al., 2014), increased irrigation water withdrawal leads to further lowering of groundwater levels, hence causing greater decrease in stream-aquifer flows. In this study, the analysis of NI and IR periods showed that since the 1970’s overall streamflow/baseflow has fallen substantially (approximately 20%) in the LFR and its tributaries. Moreover, the analysis of 1-day and 7-day low flows and FDC showed that the frequency of low flows has increased during IR period. The tributaries (gaging stations C and D) of the Flint River have shifted from perennial streams to intermittent, which suggests that groundwater withdrawals have intensified low flows levels in this region.

In this study, a systematic elimination approach was employed to eliminate the influence of climatic factors from the anthropogenic factors on flow levels. Analysis of the regional climate data revealed no significant changes in rainfall amounts between NI and IR periods for the El Niño or La Niña phases or on an overall basis, negating the influence of climate on streamflow levels during these two periods. The analysis of NI and IR periods along with ENSO showed that flow levels have not changed during El Niño phases, however, flow levels have reduced substantially during La Niña phases associated with IR period (except station D).

The comparison of NI and IR period flow levels during growing and non-growing seasons provided interesting results where non-growing season flow levels were similar during both the phases of ENSO. However, during the growing season, flow levels have dropped substantially during La Niña phases, which suggests that the combination of groundwater removal (irrigation pumpage) and La Niña induced drought have significant impact on flow levels in the LFR. While it is not surprising that a combination of drought and irrigation would negatively affect flow levels, what is surprising is the size of the effect, which in some cases was as large as 50% reduction. Lowering of stream flows due to drought and pumpage results in anoxic conditions that threaten federally-protected mussel species and other aquatic species residing in the LFR.

The systematic elimination approach undertaken in this study avoids the need for using complex, data intensive groundwater/surface water models for studying climate and anthropogenic influences on stream-aquifer interactions and can be replicated easily in other data scarce watersheds. Understanding the climate induced droughts and resulting lowering of flow levels can provide a clear picture of hydrologic droughts which might be further exacerbated in the future by increased water demand by growth in population, increased irrigated agriculture and urban sprawl. In addition to anthropogenic stress (such as population growth) on fresh water resources, it is projected that natural stresses such as extreme climatic events including drought are going to be a common phenomenon under global climate change scenarios (Easterling et al., 2000; Herring et al., 2015). Therefore, policymakers and water managers in this region should try to devise policy where limited freshwater resources can be shared between human and aquatic biota of the ecosystem.

Conflict of interest

Authors whose names are listed above certify that they have no affiliations with or involvement in any organization or entity with any financial interest or non-financial interest in the subject matter or materials discussed in this manuscript.

Acknowledgments

The authors wish to acknowledge the funding provided by the National Integrated Drought Information System (NIDIS), the National Oceanic and Atmospheric Agency (NOAA), Sectoral Applications Research Program (SARP), and the NOAA Regional Integrated Sciences and Assessments (RISA) Program for this study.

References

Aceituno, P., 1992. El Niño, the southern oscillation, and ENSO: confusing names for a complex ocean-atmosphere interaction. Bull. Am. Meteorol. Soc. 73, 483–485.
Beebee, R.A., Manga, M., 2004. Variation in the relationship between snowmelt runoff in oregon and ENSO and PDO. J. Am. Water Resour. Assoc. 40, 1011–1024.
Boulton, A.J., Hancock, P.J., 2006. Rivers as groundwater-dependent ecosystems: a review of degrees of dependency, riverine processes and management implications. Aust. J. Bot. 54, 133–144.
Bunn, S.E., Arthington, A.H., 2002. Basic principles and ecological consequences of altered flow regimes for aquatic biodiversity. Environ. Manage. 30, 492–507, http://dx.doi.org/10.1007/s00267-002-2737-0.
Chen, W.Y., 1982. Assessment of Southern Oscillation sea-level pressure indices. Mon. Weather Rev. 110, 800–807.
Chiew, F.H.S., Piechota, T.C., Dracup, J.A., McMahon, T.A., 1998. El Niño/Southern Oscillation and Australian rainfall, streamflow, and drought: links and potential for forecasting. J. Hydrol. 204, 138–149.
Diaz, H.F., Markgraf, V., 1992. El Niño: Historical and Paleoclimatic Aspects of the Southern Oscillation. Cambridge University Press.
Easterling, D.R., Meehl, G.A., Parmesan, C., Changnon, S.A., Karl, T.R., Mearns, L.O., 2000. Climate extremes: observations, modeling, and impacts. Science 289, 2068–2074, http://dx.doi.org/10.1126/science.289.5487.2068.
Eckhardt, K., 2005. How to construct recursive digital filters for baseflow separation? Hydrol. Processes 19 (2), 507–515.
Enfield, D.B., Mestas-Nuez, A.M., Trimble, P.J., 2001. The Atlantic multi-decadal oscillation and its relation to rainfall and river flows in the continental US. Geophys. Res. Lett. 28 (10), 2077–2080.
Golladay, S.W., Gagon, P., Kearns, M., Battle, J.M., Hicks, D.W., 2004. Response of freshwater mussel assemblages (Bivalvia:Unionidae) to record drought in the Gulf Coastal Plain of southwest Georgia. J. North Am. Benthol. Soc. 23, 494–506.
Gurdak, J.J., Hanson, R.T., McMahon, P.B., Bruce, B.W., McCray, J.E., Thyne, G.D., Reedy, R.C., 2007. Climate variability controls on unsaturated water and chemical movement, high plains aquifer, USA. Vadose Zone J. 6, 533–547.
Hansen, D.V., Maul, G.A., 1991. Anticyclonic current rings in the eastern tropical Pacific Ocean. J. Geophys. Res. 96 (C4), 6965–6979.
Hansen, J., Jones, J., Irmak, A., Royce, F., 2001. El Niño-Southern Oscillation Impacts on Crop Production in the Southeast United States, vol. 63. ASA Special Publication, pp. 55–76.
Harrison, K.A. 2009. Georgia Irrigation Survey – 2008. CES Misc. Pub. January 22, 2009. Athens, GA.
Herring, S.C., Hoerling, M.P., Kossin, J.P., Peterson, T.C., Stott, P.A., Eds., 2015. Explaining Extreme Events of 2014 from a Climate Perspective. Bull. Am. Meteorol. Soc., 96 (12), pp. S1–S172.
Hettmansperger, T.P., McKean, J.W., 2011. Robust Nonparametric Statistical Methods, Volume 119 of Monographs on Statistics and Applied Probability, second ed. CRC Press, Boca Raton, FL.
Hicks, D.W., Gill, H.E., Longsworthm, S.A., 1987. Hydrogeology, Chemical Quality, and Availability of Ground Water in the Upper Floridan Aquifer, Albany Area. U.S. Geological Survey; Water-Resources Investigations Report 87–4145; 31 p.
IPCC (Intergovernmental Panel on Climate Change), 2001. Climate change 2001: impacts, adaptations, and vulnerability. In: Contribution of Working Group II to the Third Assessment Report of the Intergovernmental Panel on Climate Change. Cambridge University Press, Cambridge.
Jaeckel, L.A., 1972. Estimating regression coefficients by minimizing the dispersion of the residuals. Ann. Math. Stat. 43, 1449–1458.
Johnson, N.T., Martinez, C.J., Kiker, G.A., Leitman, S., 2013. Pacific and Atlantic sea surface temperature influences on streamflow in the Apalachicola–Chattahoochee–Flint river basin. J. Hydrol. 489, 160–179.
Jones, L.E., Torak, L.J., 2006. Simulated effects of seasonal ground-water pumpage for irrigation on hydrologic conditions in the lower Apalachicola–Chattahoochee–Flint River Basin, southwestern Georgia and parts of Alabama and Florida, 1999–2002: U.S. Geological Survey Scientific Investigations Report 2006-5234, 115 p., a Web-only publication at http://pubs.usgs.gov/sir/2006/5234/.
Jordan, J.L., Wolf, A.T., 2006. Interstate Water Allocation in Alabama, Florida, and Georgia: New Issues, New Methods, New Models. University Press of Florida.
Kahya, E., Dracup, J.A., 1993. US streamflow patterns in relation to the El Niño/Southern Oscillation. Water Resour. Res. 29 (8), 2491–2503.
Keener, V.W., Ingram, K.T., Jacobson, B., Jones, J.W., 2007. Effects of El-Niño/Southern Oscillation on simulated phosphorus loading. Trans. ASABE 50 (6), 2081–2089.
Kiladis, G.N., Diaz, H.F., 1989. Global climate anomalies associated with extremes in the Southern Oscillation. J. Clim. 2 (9), 1069–1090.
Kloke, J.D., McKean, J.W., Rashid, M., 2009. Rank-based estimation and associated inferences for linear models with cluster correlated errors. J. Am. Stat. Assoc. 104 (485), 384–390.
Kulkarni, J.R., 2000. Wavelet analysis of the association between the southern oscillation and the Indian summer monsoon. Int. J. Climatol. 20, 89–104.
Lehmann, E.L., Casella, G., 1998. Theory of point estimation. In: Springer Texts in Statistics, second ed. Springer-Verlag, New York.
Lim, K.J., Engel, B.A., Tang, Z., Choi, J., Kim, K., Muthukrishnan, S., Tripathy, D., 2005. Web GIS-based hydrograph analysis tool, WHAT. JAWRA 41 (6), 1407–1416.
McCabe, G.J., Dettinger, M.D., 1999. Decadal variations in the strength of ENSO teleconnections with precipitation in the western United States. Int. J. Climatol. 19 (13), 1399–1410.
McKean, J., Schrader, R., 1980. The geometry of robust procedures in linear models. J. R. Stat. Soc. Ser. B (Methodol) 42 (3), 366–371.

Mearns, L.O., Giorgi, F., Shields, C., McDaniel, L., 2003. Climate scenarios for the southeastern US based on GCM and regional modeling simulations. Clim. Change 60, 7–36.
Mitra, S., Srivastava, P., Singh, S., Yates, D., 2014. Effect of ENSO-induced climate variability on groundwater levels in the lower Apalachicola-Chattahoochee-Flint River Basin. Trans. ASABE 57 (5), 1393–1403.
Mosner, M.S., 2002. Stream-Aquifer Relations and the Potentiomentric Surface of the Upper Floridan Aquifer in the Lower Apalachicola-Chattahootchee-Flint River Basin in Parts of Florida, Georgia, and Alabama, 1990–1998. U.S. Geological Survey; Water-Resources Investigations Report 02–4244; Atlanta, GA; 45 p.
Opsahl, S.P., Chapal, S.E., Hicks, D.W., Wheeler, C.K., 2007. Evaluation of ground-water and surface-water exchanges using streamflow difference analyses. J. Am. Water Resour. Assoc. 43, 1132–1141.
Piechota, T.C., Dracup, J.A., 1999. Long-range streamflow forecasting using El Niño- Southern Oscillation indicators. J. Hydrol. Eng. 4 (2), 144–151.
Pierce, R., Barber, R., Stiles, H.R., 1984, Georgia Irrigation, 1970–1980: A decade of growth, U.S. Geological Survey Water-Resources Investigations Report, 83-4177, 29 p.
Postel, S.L., Daily, G.C., Ehrlich, P.R., 1996. Human appropriation of renewable fresh water. Science 271 (5250), 785–788.
Pringle, C.M., Triska, F.J., 2000. Emergent biological patterns and surface-subsurface interactions at landscape scales. In: Jones, J.B., Mulholland, P.J. (Eds.), Stream and Groundwaters. Academic Press, San Diego, pp. 167–193.
Quinn, W.H., 1994. Monitoring and predicting el Niño invasions. J. Appl. Meteorol. 9, 20–28.
Rajagopalan, B., Lall, U., 1998. Interannual variability in western US precipitation. J. Hydrol. 210, 51–67.
Ropelewski, C.F., Jones, P.D., 1987. An extension of the Tahiti-Darwin Southern Oscillation Index. Mon. Weather Rev. 115, 2161–2165.
Rose, S., 2009. Rainfall runoff trends in the southeastern USA: 1938–2005. Hydrol. Processes 23, 1105–1118.
Roy, S.S., 2006. The impacts of ENSO, PDO, and local SSTs on winter precipitation in India. Phys. Geogr. 27 (5), 464–474.
Rugel, K., Jackson, C.R., Romeis, J.J., Golladay, S.W., Hicks, D.W., Dowd, J.F., 2011. Effects of irrigation withdrawals on streamflows in a karst environment: lower Flint River Basin, Georgia, USA. Hydrol. Processes 26, 523–534, http://dx.doi.org/10.1002/hyp.8149.
Schmidt, N., Luther, M.E., 2002. ENSO impacts on salinity in Tampa Bay, Florida. Estuaries Coasts 25 (5), 976–984.
Seager, R., Tzanova, A., Nakamura, J., 2009. Drought in the southeastern United States: causes, variability over the last millennium, and the potential for future hydroclimate change. J. Clim. 22, 5021–5045, http://dx.doi.org/10.1175/2009JCLI2683.1.
Seneviratne, S.I., Nicholls, N., Easterling, D., Goodess, C.M., Kanae, S., Kossin, J., Luo, Y., Marengo, J., McInnes, K., Rahimi, M., Reichstein, M., Sorteberg, A., Vera, C., Zhang, X., 2012. Changes in climate extremes and their impacts on the natural physical environment. In: Field, C.B., Barros, V., Stocker, T.F., Qin, D., Dokken, D.J., Ebi, K.L., Mastrandrea, M.D., Mach, K.J., Plattner, G.-K., Allen, S.K., Tignor, M., Midgley, P.M. (Eds.), Managing the Risks of Extreme Events and Disasters to Advance Climate Change Adaptation. Cambridge University Press, Cambridge, UK, and New York, NY, USA, pp. 109–230, A Special Report of Working Groups I and II of the Intergovernmental Panel on Climate Change (IPCC).
Shah, T., Molden, D., Sakthivadivel, R., Seckler, D., 2000. The Global Groundwater Situation: Overview of Opportunities and Challenges. International Water Management Institute, Colombo, Sri Lanka, pp. 21.
Singh, S., Srivastava, P., Abebe, A., Mitra, S., 2015. Baseflow response to climate variability induced droughts in the Apalachicola–Chattahoochee–Flint River Basin, U.S.A. J. Hydrol. 528, 550–561.
Stanford, J.A., Ward, J.V., 1993. An ecosystem perspective of alluvial rivers: connectivity and the hyporheic corridor. J. North Am. Benthol. Soc. 12, 48–60.
Tootle, G.A., Piechota, T.C., Singh, A., 2005. Coupled oceanic–atmospheric variability and US streamflow. Water Resour. Res. 41, 1–11.
Trenberth, K.E., Stepaniak, D.P., 2001. Indices of El Niño evolution. J. Clim. 14, 1697–1701.
Trenberth, K.E., 1997. The definition of El Niño. Bull. Am. Meteorol. Soc. 78, 2771–2777.
Troup, A.J., 1965. The 'southern oscillation'. Q. J. R. Meteorolog. Soc. 91, 490–506.
U.S. Fish & Wildlife Service and Environmental Protection Agency (USFWS and EPA). 1999. Instream flow guidelines for the ACT and ACF Basins interstate water allocation formula. Enclosure to letter dated October 25, 1999, from J.H. Hankinson, EPA Regional Administrator, and S.D. Hamilton, USFWS Regional Director, to L. Thomas, ACF Federal Commissioner. 14 pp. + appendices.
Winter, T.C., Harvey, J.W., Franke, O.L., Alley, W.M., 1998. Ground Water and Surface Water: A Single Resource. U.S. Geological Survey Circular, 1139; Denver, CO; 4 p.
Woessner, W.W., 2000. Stream and fluvial plain ground water interactions: rescaling hydrogeologic thought. Ground Water 38, 423–429.
Wolter, K., Timlin, M.S., 1993. Monitoring ENSO in COADS with a seasonally adjusted principal component index. Proc 17th Climate Diagnostics Workshop, 52–57.